# Proposal of new indicator ”Red Tide Index” for the Seto Inland Sea, Japan

Ishii, Daisuke
Research Institute for Applied Mechanics, Kyushu University

Yanagi, Tetsuo
Research Institute for Applied Mechanics, Kyushu University

Sasakura, Satoshi
Idea Inc.

https://doi.org/10.15017/27155

出版情報：九州大学応用力学研究所所報. 144, pp.1-11, 2013-03. Research Institute for Applied Mechanics, Kyushu University
バージョン：

# Proposal of new indicator "Red Tide Index" for the Seto Inland Sea, Japan

Daisuke ISHII[*1], Tetsuo YANAGI[*1] and Satoshi SASAKURA[*2]

E-mail of corresponding author: *dishii@riam.kyushu-u.ac.jp*

(Received January 31, 2013)

**Abstract**

We propose a new indicator, the Red Tide Index, which permits assessment of spatial and temporal scales and impacts of red tide. By examining temporal and spatial variations of this index across the entire Seto Inland Sea area, we can assess regional characteristics of its coastal and offshore areas. The index for Osaka Bay was the highest in the sea, but it has markedly declined in recent years. This suggests that water quality in the bay has recovered. In areas with high (low) Red Tide Index density, dissolved oxygen concentration in the bottom layer is low (high).

**Key words** : *Red Tide Index, spatial-temporal variation of red tide, coastal area, offshore area, the Seto Inland Sea*

## 1. Introduction

The Seto Inland Sea (Fig. 1) is surrounded by three large islands, Honshu, Shikoku, and Kyushu, and is near the center of the Japanese archipelago. It is the largest semi-enclosed coastal sea in Japan. It connects with the Pacific Ocean via the Kii and Bungo Channels, and with the Japan Sea via the Kanmon Strait. It has bountiful marine resources and scenic beauty.

However, water quality in the sea has been worsened by human activities associated with the rapid economic growth of Japan since the 1960s. Increased pollutant loading from land, excessive reclamation works in coastal areas, and large-scale sea sand mining have seriously damaged the marine environment. Red tides and oxygen-deficient water masses have been frequent every summer, and the fish catch has drastically decreased (Kamizono *et al.*, 1996a[1]; Yamada and Kajiwara, 2004[2]).

To solve such problems, the "Law Concerning Special Measures for Conservation of the Environment of the Seto Inland Sea" was enacted in 1978. Under the umbrella of this special law, total load control of TP (total phosphorus) and TN (total nitrogen) from land-based sources was begun. However, TP and TN concentrations did not change in the Seto Inland Sea, except in Osaka Bay. This is because existing TP and TN in the sea (except the bay) does not chiefly originate from land but from the Pacific Ocean (Yanagi, 1997[3]; Yanagi and Ishii, 2004[4]). TP and TN concentrations have decreased in the bay with application of the total TP and TN load control law, because the ratios of TP and TN from land are about 60% to 70%, respectively (Ishii and Yanagi, 2004[5]).

In addition to Osaka Bay, water environments are different in coastal and offshore areas in other regions of the Seto Inland Sea (Ishii and Yanagi, 2005[6]). To clarify water environment characteristics in each area of the sea, we propose a new indicator, the "Red Tide Index" (RI), which is capable of assessing spatiotemporal scales and impacts of red tide. We assess water environment characteristics in each area of the sea by examining spatial and temporal variations in RI.

## 2. Basic data and various definitions

### 2.1 Material of red tides

The Seto Inland Sea Fisheries Coordination Office of the Fisheries Agency, Ministry of Agriculture, Forestry and Fisheries of Japan has annually collected and organized various data concerning red tide in the Seto Inland Sea since 1970. An annual report entitled "Red Tides in the Seto Inland Sea" (hereafter, the "red tide report") has been published annually. Detailed and valuable information on red tide occurrence has been recorded in this report, such as names of affected sea

*1 Research Institute for Applied Mechanics (RIAM), Kyushu University

*2 Ides Incorporated

regions, distributions, frequency, phytoplankton species, starting and ending days, and duration.

We analyzed spatiotemporal variations and characteristics of red tides in each sea region, based on data such as the name of the affected region, occurrence distribution (area) and duration. These data were all published in the red tide report from 1979 to 2004 (Fisheries Agency, 1980–2005[7]).

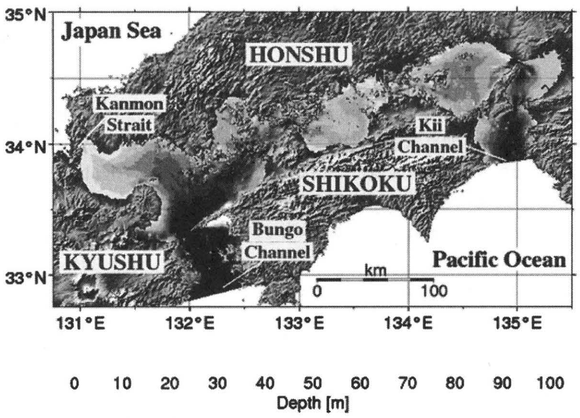


Fig.1 The Seto Inland Sea, Japan

## 2.2 Definition of Red Tide Index

Information such as incidents of red tide and fishery damage has often been used as an evaluation tool apart from water quality, to determine water environment characteristics in some coastal areas. However, the frequency of red tides is not necessarily related to their temporal and spatial scales and damages. This limits the discourse on these scales and impacts.

Tsutsumi *et al.* (2003)[8] proposed a "red tide scale index" to represent temporal and spatial scales of red tide occurrences in Ariake Bay, where they have recently become a problem to society. Using this index, they discuss the "increasing scale of red tide," which cannot be revealed by analyzing observed data of water quality and number of occurrences. There have been many analyses of various water quality data and red tide incidents in the Seto Inland Sea. However, there are no studies using the above approach to assess the spatiotemporal scales and impacts of red tide in the sea.

In this paper, we apply concepts similar to Tsutsumi *et al.* (2003)[8] for the sea, and calculate RI (=S×DAY), which is expressed as an area (S) multiplied by duration (DAY) of red tides (all of which have been recorded in the red tide report).

## 2.3 Definition of the coastal and offshore area

It has been estimated that the majority of existing TP and TN in the Seto Inland Sea, except Osaka Bay, originates from the Pacific Ocean (Yanagi and Ishii, 2004[4]; Ishii and Yanagi, 2004[5]). In the coastal area of the sea, there is direct inflow of large land-derived loads; such loads may affect water quality there (Ishii and Yanagi, 2005[6]). This indicates that the severity of land-derived pollution differs between coastal and offshore areas. Hence, it is important to separate these areas when assessing red tide characteristics.

Two characteristic ranges were defined, a "coastal area" and an "offshore area." As shown in Fig. 2, we divided all bays and basins of the Seto Inland Sea into a rectangular mesh, with a size of two minutes in longitude and latitude (about 3.1 km in the east-west direction, and 3.7 km north to south). We defined the coastal areas as those within one or two mesh squares from land, and offshore areas as those excluding the coastal areas in all bays and basins. The "entire area" includes both coastal and offshore areas of the sea.

Water areas (Fig. 3(a)) and their ratios (Fig.3(b)) for 12 sea regions are calculated using a Geographic Information System (GIS). These regions are the Kii Channel, Osaka Bay, Harima-Nada, Bisan-Seto, Bingo-Nada, Hiuchi-Nada, Aki-Nada, Hiroshima Bay, Iyo-Nada, Beppu Bay, Suo-Nada, and Bungo Channel (Fig. 2). According to this analysis for the entire Seto Inland Sea (about 22,700 $km^2$), coastal areas occupy about 37% (about 8,500 $km^2$), and offshore ones about 63% (about 14,200 km2). Beppu Bay (about 83%) and Bisan-Seto (about 63%) have especially high proportions of coastal area, whereas Iyo-Nada (about 21%) and Hiuchi-Nada (about 29%) have low proportions.

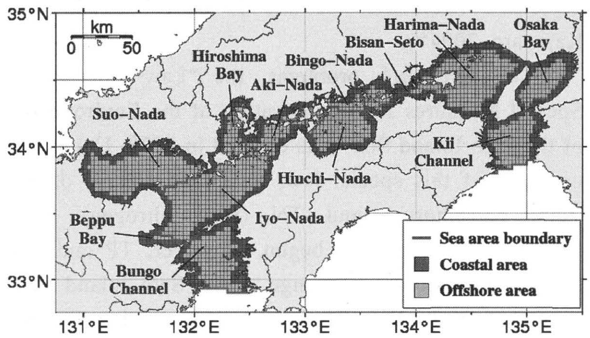


Fig.2 Classification of sea areas into coastal and offshore for the Seto Inland Sea

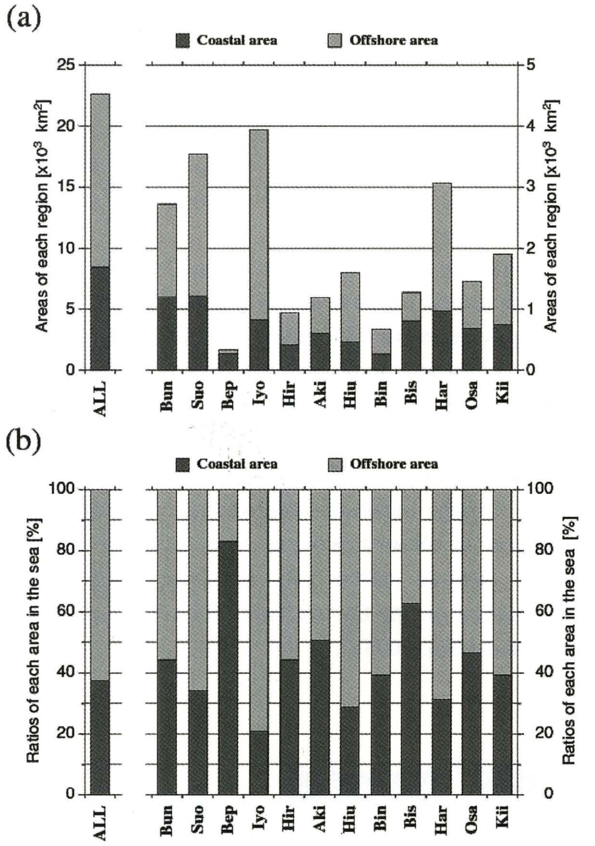


Fig.3 Sea areas (a) and ratios for 12 regions of coastal and offshore areas (b) to total the Seto Inland Sea area, calculated by GIS

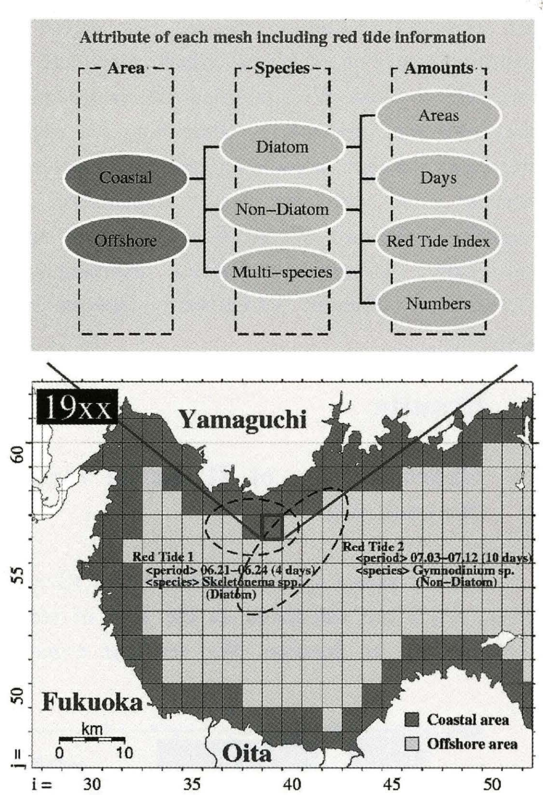


Fig.4 Schematic diagram of frequency of annual red tide around Suo-Nada and mesh attributes, including red tide information, incorporated into GIS for red tide basic dataset

## 2.4 Construction of red tide basic dataset and RI assessment method

To derive the RI using data from the red tide report, we assembled a spatiotemporal dataset of various red tide quantities. In this approach, we used GIS, whose introduction and spread began in earnest around 1995. This was because of promotion of the National Spatial Data Infrastructure, mainly by the Japanese government.

Part of the information from the red tide report was digitized. There were instances in which red tide distribution (area) had not been quantified. After first tracing the red tide distribution map for a certain year in the red tide report, it was quantified by importing the information into the GIS. With this map, information on the phytoplankton species comprising the red tide, its area and duration, number of cases and RI were converted to spatial digital data. By means of the spatial division mentioned above, we constructed the red tide basic dataset for each year, with attributes related to the red tide partitioned and collected into the 2-minute mesh squares (Fig. 4).

When various red tide information within a mesh square is superimposed, this method (Fig. 4) produces the most valuable features for differentiating attributes. Table 1 shows a concrete example of the calculation method for various red tide quantities transformed into GIS.

Table 1 Example of annual red tide basic data collection for mesh square M (39, 57), as shown in Fig. 4 (D – diatom, ND – non-diatom, M – multi-species)

| Year [ 19xx ] | | M (39, 57) Suo-Nada | | Specific area [ Coastal ] | | | |
|---|---|---|---|---|---|---|---|
| Types | | S [km$^2$] | | DAY [day] | | RI [km$^2$ day] | |
| D | total | 11.47 | 17.21 | 4 | 14 | 45.88 | 103.23 |
| ND | | 5.74 | | 10 | | 57.35 | |
| M | | 0 | | 0 | | 0 | |

The basic dataset was constructed for each year with attributes relating to the red tide, which were quantified yearly on each mesh square for the 26 years from 1979 to 2004. We simplified the classification of many phytoplankton species comprising red tide into three types – diatom, non-diatom, and multi-species – to construct a red tide basic dataset. Explanation of the simplified definition of red tide component species classification is omitted, because assessment and discussion of different phytoplankton species is not given here.

## 3. Results

### 3.1 Characteristics of RI spatial variation for each year

Figure 5 shows spatial distributions of RI (1979–2004), which are calculated as the area of red tide multiplied by its duration. We see that a red tide occurred every year in a broad area in the eastern part of Osaka Bay (its head). As represented by the extremely high RI in 1982 and 1992, scales of red tide in this bay had pronounced spatial characteristics relative to other regions. In the western part of the bay, there were years (1992, 2002, and 2003) with almost no red tide throughout the year.

Although not on the same scale as Osaka Bay, there are regions that had remarkably high RI. These include Harima-Nada, eastern Hiuchi-Nada, northern Hiroshima Bay, Suo-Nada, and Beppu Bay (Fig. 5). Especially large red tide areas covered the entire Harima-Nada region in 1983, 1989, 2001, and 2004, and the entire Suo-Nada region in 1985 and 1986. There was resultant fishery damage (death of cultured fishery products and color loss in cultured seaweed), and losses of between several hundred million yen and several billion yen (Association for the Environmental Conservation of the Seto Inland Sea, 2006)[9].

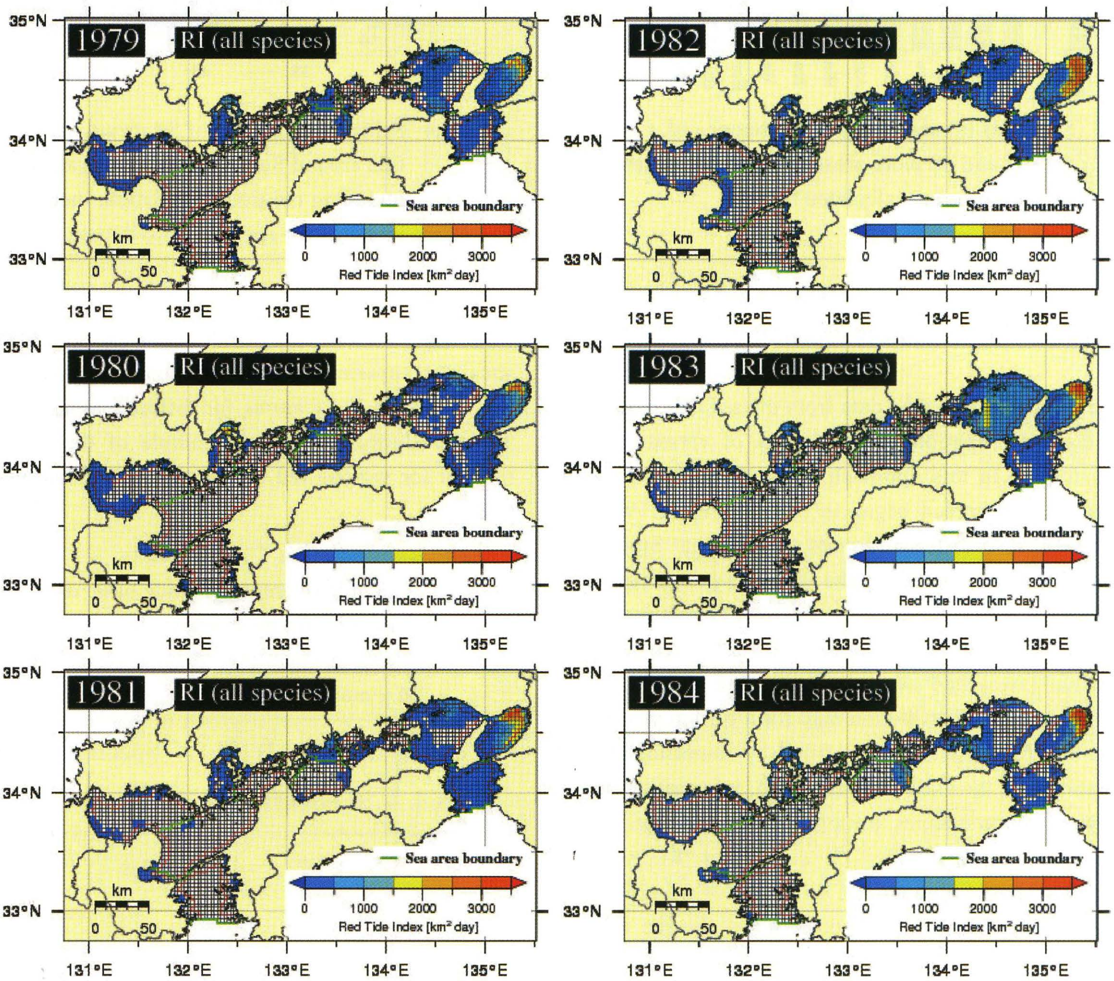


Fig.5 Spatial distributions of Red Tide Index in the Seto Inland Sea, from 1979 to 2004. (1979–1984)

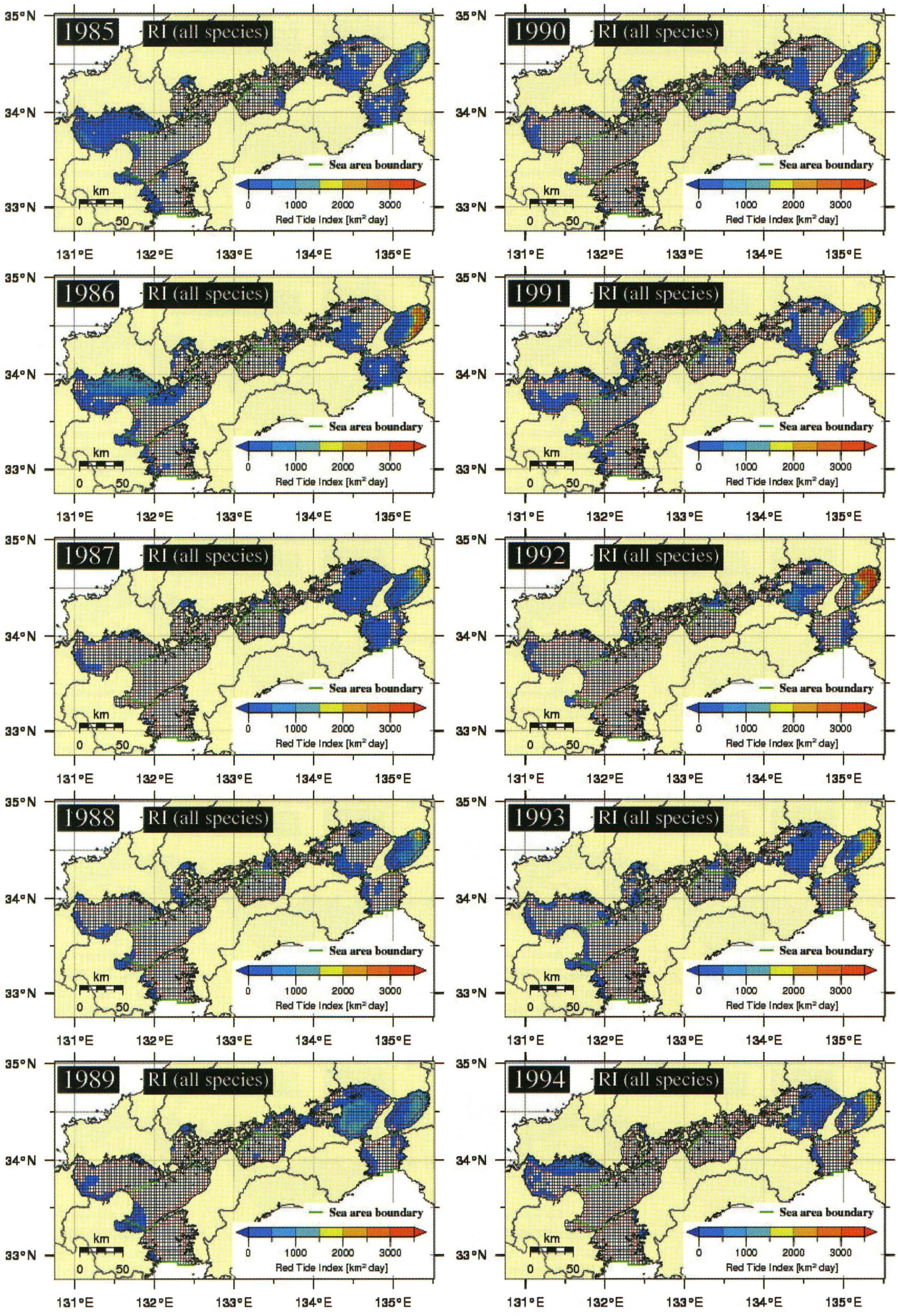


Fig.5 Continued. (1985–1994)

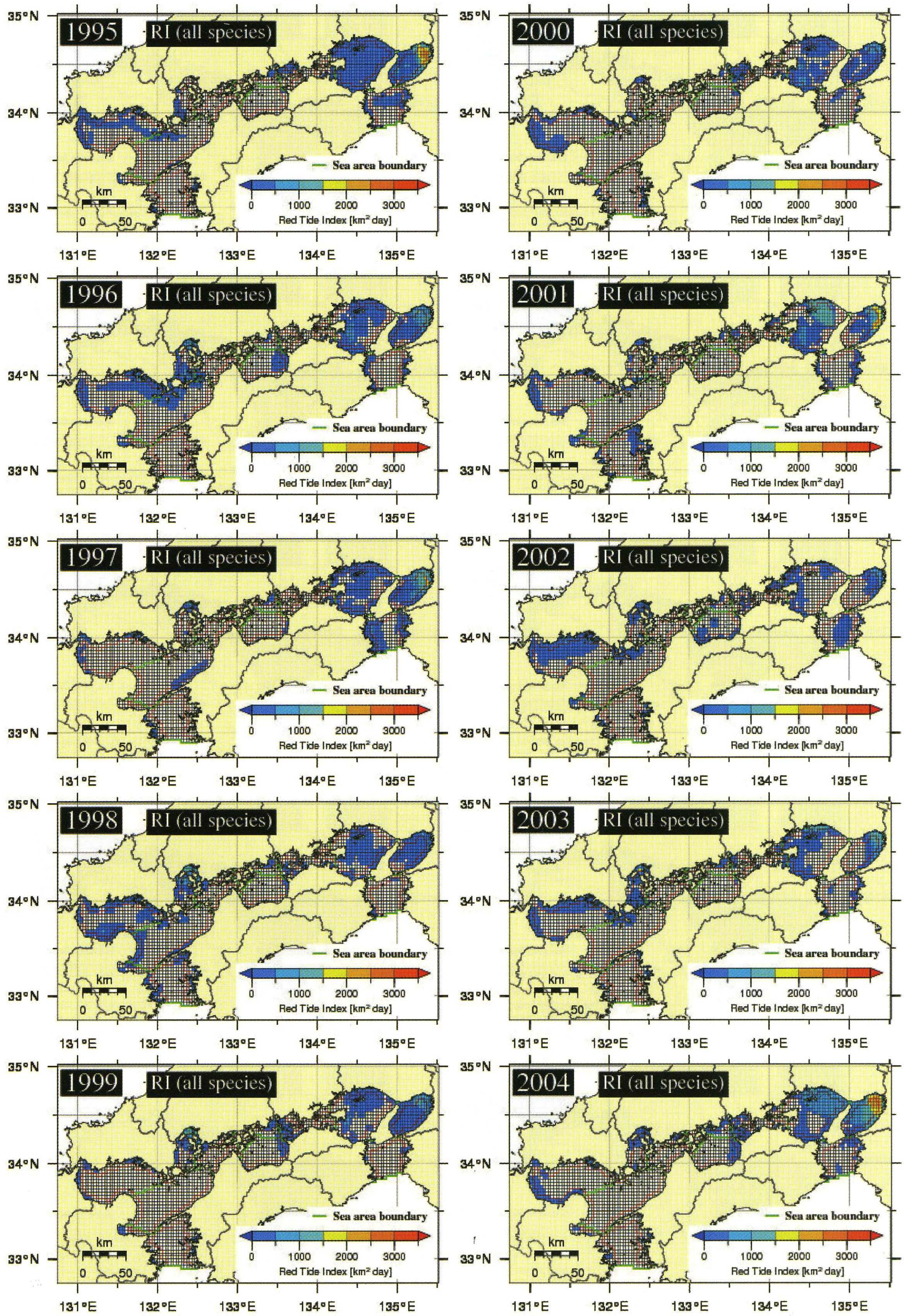


Fig.5 Continued. (1995–2004)

## 3.2 RI variability characteristics and time averages for each period

To evaluate average red tide distribution, features and differences over specified periods, we divided the data analysis period (1979–2004; 26 years) in two – Period I (1979–1991; mainly the 1980s) and Period II (1992–2004; from the 1990s to the first half of the 2000s). Subsequently, we focused on spatiotemporally averaged RI features within each period and red tide variation with area and period.

Figure 6 shows RI spatial distribution in the Seto Inland Sea, averaged by period. Figure 7(a–c) shows the RI of Fig. 6 spatially averaged over the specific areas (coastal, offshore, and entire) defined in Section 2.3. Figure 7(d–f) shows RI normalized by dividing these values by each specific area (RI density). "ALL-Osa" at the upper left of Fig. 7 refers to 11 regions of the Seto Inland Sea, except Osaka Bay.

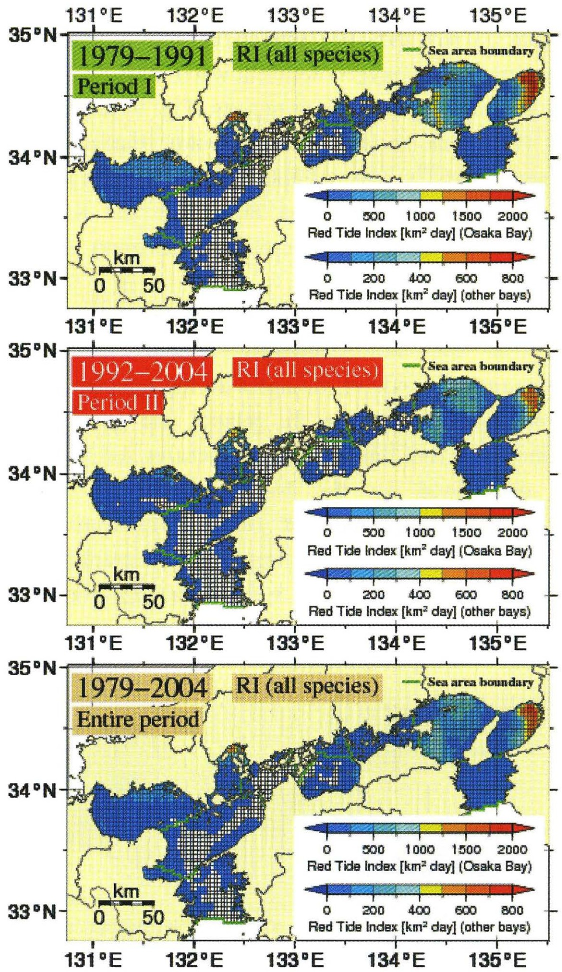


Fig.6 Spatial distributions of Red Tide Index, time-averaged for each period (upper panels for Period I (1979–1991), middle panels for Period II (1992–2004), lower panels for entire period (1979–2004))

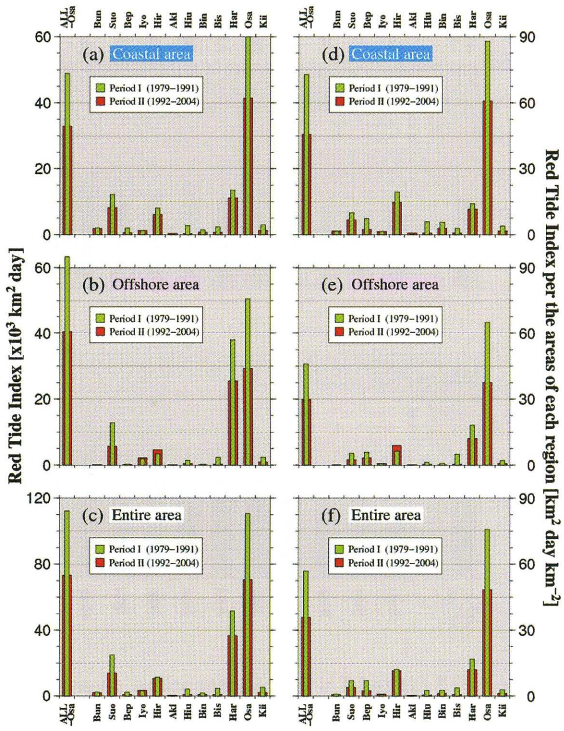


Fig.7 Red Tide Index (a–c) and Red Tide Index density (d–f), averaged over specific areas and periods (upper panels for coastal area, middle panels for offshore area, lower panels for entire area)

As shown in Figs. 6 and 7, the RI for Osaka Bay is extremely high relative to other coastal and offshore areas. Indeed, in the coastal areas of the bay, it is higher than the sum of RI for the 11 regions (ALL-Osa) excluding the bay (Fig. 7(a)). The region with the second highest RI is neighboring Harima-Nada. The characteristics in Harima-Nada contrast with those in Osaka Bay, with offshore area RI greater than that of the coastal area. The Harima-Nada RI in its coastal areas (10,600–14,500 km$^2$ day) is about one quarter that of Osaka Bay (42,500–60,400 km$^2$ day). In its offshore areas, this proportion is about 80%. For RI densities, there is no notable difference between Harima-Nada coastal and offshore areas, but there is a clear difference between Osaka Bay and Harima-Nada (Fig. 7(d–f)). The RI and RI density for Hiuchi-Nada are not evident in Fig. 7, but Figure 5 shows that there was extensive red tide almost every year around the southeastern part of its coastal area.

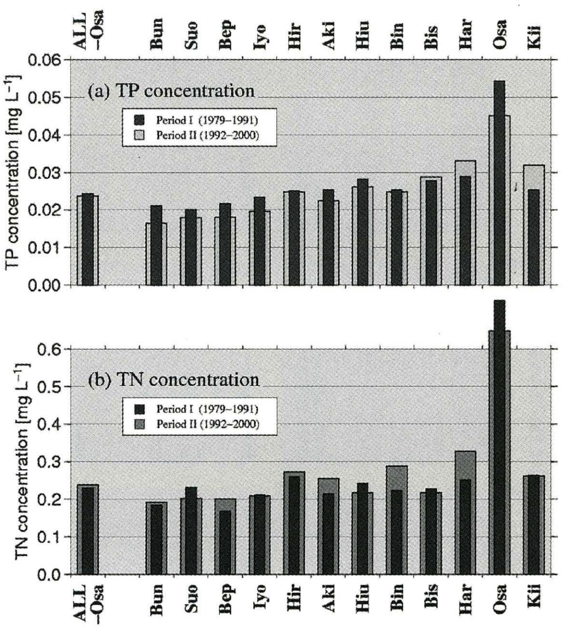


Fig.8 TP (a) and TN (b) concentrations, averaged over each period and region (from wide-area water quality monitoring by Ministry of the Environment)

Figure 8 depicts spatial distributions of TP and TN concentrations for water quality monitoring over a wide area of the Seto Inland Sea, averaged by period. Nutrient concentration in the Kii Channel is as high as Harima-Nada (Fig. 8), but the RI is about the same as in other areas with low nutrient concentrations (Fig. 7). In the Kii Channel, there are large variations in the current, nutrient and biological production (ecosystem) environments, because of the onshore/offshore movement of the Kuroshio current (Takashi *et al.*, 2006[10]; Ue, 2006[11]). This means that the frequency and scale of red tides in the channel are affected by the physical as well as the nutrient environment. Similar findings have been reported in numerical analysis studies using a marine ecosystem model (Hayashi and Yanagi, 2007[12]; Hayashi and Yanagi, 2008[13]).

Apart from the aforementioned areas, Suo-Nada, Hiroshima Bay, and Beppu Bay in the western Seto Inland Sea had RIs increasing in the order listed (Fig. 7(a–c)). However, Hiroshima Bay had the highest RI density of the three areas (Fig. 7(d–f)). This suggests that the potential for red tide in that bay is the greatest in the western part of the sea.

The RI and RI density for the three areas (coastal, offshore, and entire) in Period I (1979–1991) and Period II (1992–2004) show a decreasing trend (except for the offshore areas of Hiroshima Bay and Iyo-Nada). Such a trend, which varies by region, does not correspond well to those of TP and TN concentrations (Fig. 8). This suggests that the primary production environments are unique in each region (Hayashi and Yanagi, 2002[14]; Yara and Yanagi, 2004[15]; Yamamoto and Hashimoto, 2007[16]).

## 4. Discussion

High RI regions of Osaka Bay, Harima-Nada, Hiuchi-Nada, Hiroshima Bay and Suo-Nada with frequent red tides correspond well with regions of low dissolved oxygen (DO) concentration in the bottom layer.

Based on long-term observation data from water quality monitoring over wide regions, spatiotemporal variations of DO concentration in the bottom layer of the Seto Inland Sea were clarified by Yanagi and Ishii (2008)[17]. They indicated that in regions of low DO concentration, an oxygen-deficient water mass (hypoxia) was generated yearly. These regions (Fig. 9) are Osaka Bay (Nakajima *et al.*, 2007[18]), central Harima-Nada (Yanagi, 1996[19]), eastern Hiuchi-Nada (Takeoka *et al.*, 1986[20]), northern Hiroshima Bay (Date and Kiyoki, 2006[21]), and southwest Suo-Nada (Kamizono *et al.*, 1996b[22]).

We assessed the relationship between the RI (red tide) in the aforementioned regions and DO concentration (hypoxia), measured during summer in the bottom layer of the sea. In general, the generation, maintenance, and disappearance processes for hypoxia are determined by the balance between oxygen consumption (respiration of benthic organisms and decomposition of organic matter by bacteria) and oxygen supply (supply by vertical mixing from the

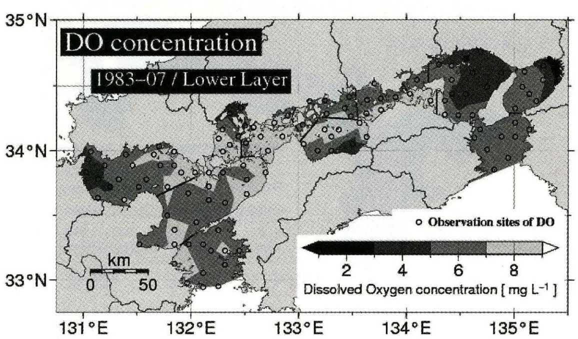


Fig.9 Spatial distribution of DO concentration, measured in July 1983 in the bottom layer of the Seto Inland Sea (from Yanagi and Ishii, 2008)[17]

surface layer and generation from photosynthesis). These vary on a time scale between several days and several weeks, owing to such factors as sediment environment, seabed topography and tidal phase, and various weather disturbances (Yanagi, 2004[23]; Yanagi and Ishii, 2009[24]).

Figure 9 shows an example of the DO concentration distribution in the bottom layer of the Seto Inland Sea during one summer (1983). These DO concentrations are low relative to other sea areas. Nevertheless, areas with concentrations significantly lower than the standard for hypoxia (3.6 mg $L^{-1}$ ; Yanagi, 1989[25]) are rare, other than Osaka Bay. Still, we examined the relationship with RI, because hypoxia is likely where DO concentration is low.

Figure 10 shows a scatter plot of summer DO concentration in the bottom layer versus annual RI density, from 1981 to 2000 for all regions in the sea. Because averaging has been done on the summer DO concentrations for each region, they do not fall below the standard for hypoxia (3.6 mg $L^{-1}$; Yanagi, 1989[25]). However, the result reveals that areas with higher (lower) RI density tend toward lower (higher) DO concentrations. We verified a statistically significant negative correlation between the two factors (correlation coefficient = −0.727, p<0.01).

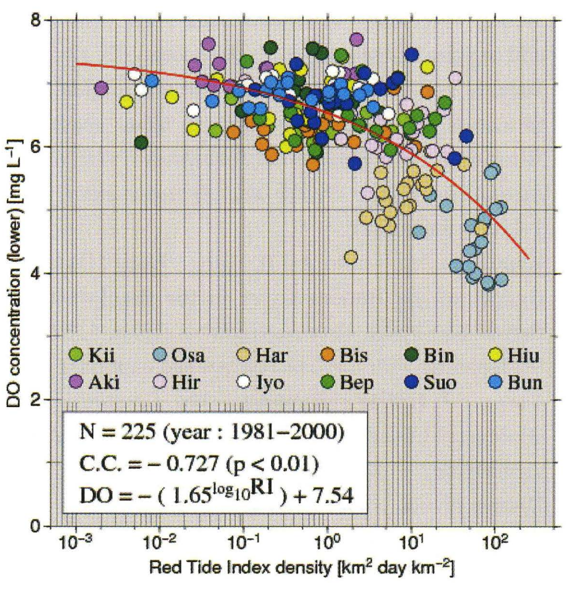


Fig.10 Relationship between Red Tide Index density and DO concentration in bottom layer of the Seto Inland Sea during summer. "N" and "C.C." refer to data numbers and correlation coefficient between RI density and DO concentration.

This indicates that the relationship between regions of red tide occurrence in the Seto Inland Sea surface layer and regions of hypoxia formation in the bottom layer is mainly determined by a vertically one-dimensional process. The red tide is generated by an extended (abnormal) growth of surface phytoplankton after their die-off and sinking, oxygen consumption with organic matter decomposition in the bottom layer, and reduced vertical oxygen supply with stratification, producing hypoxia. However, Osaka Bay (Yodo River) and Hiroshima Bay (Ota River) have dominant estuarine circulations, because of strong river inflows from land to the bay heads. There, we must consider the horizontal oxygen supply caused by this estuarine circulation (Hashimoto *et al.*, 2006[26]; Nakajima *et al.*, 2007[18]).

## 5. Conclusions

In this paper, we proposed the RI for assessing spatial and temporal scales and impacts of red tide. By examining spatiotemporal RI variations across all regions of the Seto Inland Sea, we appraised the regional characteristics of coastal and offshore areas.

We found that in comparison with other areas, the RI for Osaka Bay was higher than its sum for 11 regions (ALL-Osa) excluding that bay. The RI and RI density for the bay declined markedly in recent years. This suggests that water quality in the bay has recovered because of a decrease in its nutrient concentration.

Focusing on the connection between regions of red tide occurrence and those of hypoxia formation, we investigated the relation between the RI density and DO concentration in the bottom layer of the Seto Inland Sea. The result shows that regions with high (low) RI density had low (high) DO concentrations, with a statistically significant negative correlation between the two.

As a subject of future study, we must assess water environment characteristics in coastal and offshore areas of the entire region. This can be done by investigating spatiotemporal RI variations for each phytoplankton species and predominant red tide type in each area of the Seto Inland Sea.

## References

1) Kamizono, M., T. Eto and H. Sato (1996a) : Relationship between the Oxygen-Deficient Water Formation and Meteorological Conditions in the Southwestern Part of Suo-Nada. *Bulletin on Coastal Oceanography*, 33, 179-190. (in Japanese with English abstract and captions)

2) Yamada, M. and Y. Kajiwara (2004) :

Characteristics of Phytoplankton Occurrence in the Hyper-eutrophic Environment, Dokai Bay, Japan. *Oceanography in Japan*, 13, 281-293. (in Japanese with English abstract and captions)

3) Yanagi, T (1997) : Budgets of Fresh Water, Nitrogen and Phosphorus in the Seto Inland Sea. *Oceanography in Japan*, 6, 157-161. (in Japanese with English abstract and captions)

4) Yanagi, T. and D. Ishii (2004) : Open ocean originated phosphorus and nitrogen in the Seto Inland Sea. *J. Oceanogr.*, 60, 1001-1005.

5) Ishii. D., and T. Yanagi (2004) : C Origins and Variable Mechanisms of Total Phosphorus and Total Nitrogen Concentrations in the Seto Inland Sea. *Oceanography in Japan*, 13, 389-401. (in Japanese with English abstract and captions)

6) Ishii. D., and T. Yanagi (2005) : Changes in Total Phosphorus and Total Nitrogen Concentrations in the Coastal and Entire Areas of the Seto Inland Sea. *Oceanography in Japan*, 14, 35-45. (in Japanese with English abstract and captions)

7) Fisheries Agency (1980-2005) : Red tides in the Seto Inland Sea. *Annual Report of the Seto Inland Sea Fisheries Coordination Office*. (in Japanese)

8) Tsutsumi, H., E. Okamura, M. Ogawa, T. Takahashi, K. Yamaguchi, S. Montani, N. Kobashi, T. Adachi and T. Komatsu (2003) : Studies of the Cross Section of Water in the Innermost Areas of Ariake Bay with the Recent Occurrence of Hypoxic Water and Red Tide. *Oceanography in Japan*, 12, 291-305. (in Japanese with English abstract and captions)

9) Association for the Environmental Conservation of the Seto Inland Sea (2006) : Environmental Conservation in the Seto Inland Sea. 163pp. (in Japanese)

10) Takashi, T., T. Fujiwara, T. Sugimoto and W. Sakamoto ( 2006 ) : Prediction of slope water intrusion into the Kii Channel. *J. Oceanogr.*, 62, 105-113.

11) Ue, S. (2006) : Interannual Variations in the Ecosystem of the Kii Channel, Eastern Seto Inland Sea. *Bulletin on Coastal Oceanography*, 43, 137-142. (in Japanese with English abstract and captions).

12) Hayashi, M. and T. Yanagi (2007) : Numerical Analysis of the Change of Red Tide Species in the Yodo River Estuary by the Ecosystem Model, *Review of the Faculty of Maritime Sciences, Kobe University*, 4, 45-59. (in Japanese with English abstract and captions)

13) Hayashi, M. and T. Yanagi (2008) : Analysis of change of red tide species in Yodo River estuary by the numerical ecosystem model, *Marine Pollution Bulletin*, 57, 103-107.

14) Hayashi, M. and T. Yanagi (2002) : Comparison of the Lower Trophic Level Ecosystem with Suo-Nada and the Inner Part of Osaka Bay. *Oceanography in Japan*, 11, 591-611. (in Japanese with English abstract and captions)

15) Yara, Y. and T. Yanagi (2004) : Environmental capacity of oyster culture in the northern part of Hiroshima Bay. *Engineering sciences reports, Kyushu University*, 26, 15-22 (in Japanese with English abstract and captions)

16) Yamamoto, T. and T. Hashimoto (2007) : Estuarine Circulation and Primary Production. *Bulletin on Coastal Oceanography*, 44, 137-146. (in Japanese with English abstract and captions)

17) Yanagi, T. and D. Ishii (2008) : Oxygen-deficient water mass in the Seto Inland Sea. *"Seabed environment in the Seto Inland Sea" ed. by T. Yanagi*, Koseisha-Koseikaku Co., Ltd., 77-88.

18) Nakajima, M. and T. Fujiwara (2007) : Estuarine Circulation and Hypoxic Water Mass in Osaka Bay. *Bulletin on Coastal Oceanography*, 44, 157-163. (in Japanese with English abstract and captions)

19) Yanagi, T. (1996) : Physical processes relating to Red Tide. *"Red Tide" ed. by T.Okaichi*, Terra Scientific Publishing Company, Tokyo, 259-322.

20) Takeoka, H., T. Ochi and T. Takatani (1986) : The anoxic water mass in Hiuchi-Nada Part2. The heat and oxygen budget model. *J. Oceanogr.*, 42, 12-21.

21) Date, E. and T. Kiyoki (2006) : The distribution and formation of an oxygen-deficient water mass in Hiroshima Bay. *Reports of Hiroshima Prefectural Institute of Public Health and Environmental*, 14, 1-11. (in Japanese)

22) Kamizono, M., T. Eto and H. Sato (1996b) : Oxygen Budget of the Bottom Layer in the Southwestern Part of Suo-Nada. *Oceanography in Japan*, 5, 87-95. (in Japanese with English abstract and captions)

23) Yanagi, T (2004) : Hypoxia : The Chemical and Biological Consequences of the Mechanisms of its Generation, Maintenance, Variability and Disappearance. *Oceanography in Japan*, 13, 451-460. (in Japanese with English abstract and captions)

24) Yanagi, T. and D. Ishii (2009) : Generation and Disappearance Mechanisms of Hypoxia in the Head of Hakata Bay. *Oceanography in Japan*, 18, 169-176. (in Japanese with English abstract and captions)

25) Yanagi, T. (1989) : Hypoxia : The Chemical and Biological Consequences of the Mechanisms of its

Generation, Maintenance, Variability and Disappearance. *Bulletin on Coastal Oceanography*, 26, 141-145. (in Japanese with English abstract and captions)

26) Hashimoto, T., A. Ueda and T. Yamamoto (2006) : Influence of estuarine circulation on the biological production of the northern Hiroshima Bay, Japan, in summer season. *Bulletin of the Japanese Society of Fisheries Oceanography*, 70, 23-30. (in Japanese with English abstract and captions)